MODELING AND SIMULATION OF THERMOELECTRIC GENERATOR

BY:

UJJWAL VERMA

FAKULTÄT FÜR INFORMATIK UND ELEKTROTECHNIK

UNIVERSITY OF ROSTOCK

A REPORT SUBMITTED IN THE PARTIAL FULFILMENT OF

SOFTWARE LAB PROJECT

SEPTEMBER, 2017

UNDER THE GUIDANCE OF:

PROF. DR.-ING. DENNIS HOHLFELD

ACKNOWLEDGEMENTS

I would like to express my deep gratitude to Prof. Dr.-Ing. Dennis Hohlfeld for his guidance and continuous supervision during the software lab project. I am indebted to him for providing necessary information and motivation that led to the completion of this work. I would also like to thank Mr. Sharath Goud Yalkoti for providing with the required data to carry out this project.

Finally, I would also like to thank my parents for their support and encouragement throughout my study, this accomplishment would not have been possible without them.

ABSTRACT

This report presents a comprehensive method for modeling a thermoelectric generator utilizing Bismuth Telluride. The proposed parametric model enables easy modification to simulate different thermoelectric modules. Presently, low-power implantable devices are powered using non-rechargeable lithium batteries. In many situations it is desirable to develop autonomous implantable devices that do not require any external power input. One such alternative approach considered for internally powering autonomous implantable devices is using thermal power sources. The model in its current state can be used for further analysis such as a biomedical multiphysics simulation of electrically active implants.

Keywords: Thermoelectric generator, Bismuth Telluride, Seebeck effect

Contents

LIST OF FIGURES

LIST OF TABLES

NOMENCLATURE

N	Number of thermocouple
N'	Number of legs
T	Operating temperature (K)
$\overline{T}$	Average temperature between the hot and cold surfaces (K)
ZT	Figure of Merit
R_{el}	Electrical Resistance (Ω)
R_{th}	Thermal Resistance (K/W)
V_{out}	Output Voltage (V)
P_{max}	Maximum power output (W)
α_n	Seebeck coefficient of n-type semi-conductor (V/K)
α_p	Seebeck Coefficient of p-type semi-conductor (V/K)
κ_n	Thermal Conductivity of n-type semi-conductor (W/mK)
κ_p	Thermal Conductivity of p-type semi-conductor (W/mK)
$\kappa_{Al_2O_3}$	Thermal Conductivity of ceramic plate(W/mK)
κ_{cu}	Thermal Conductivity of copper (W/mK)
$\kappa_{mean,leg}$	Mean thermal Conductivity of p-type and n-type(W/mK)
σ_n	Electrical Conductivity of n-type semi-conductor (S/m)
σ_p	Electrical Conductivity of p-type semi-conductor (S/m)
ρ_n	Resistivity of n-type semi-conductor (Ωm)
ρ_p	Resistivity of p-type semi-conductor (Ωm)
ρ_{cu}	Resistivity of copper (Ωm)
h_{leg}	Height of peltier element leg (m)
h_{cu}	Height of copper contact (m)
$h_{Al_2O_3}$	Height of ceramic plate (m)
A_{leg}	Cross-sectional area of peltier element leg (m^2)
$A_{Al_2O_3}$	Cross-sectional area of ceramic plate leg (m^2)
$A_{cu,contact}$	Area of contact between leg and cooper contact(m^2)

ABBREVATIONS

TEG	Thermoelectric Generator
TE	Thermoelectric
TEC	Thermoelectric Cooler

1 Introduction

Energy harvesting is the process of electronically capturing and storing energy from otherwise unusable and wasted sources. More often than not, these are potential energy sources that are by product of mechanical, thermal or even biological processes [1]**.** Thermoelectric generators (TEGs), are solid state devices that facilitate recovery of lost thermal energy. Figure 1 illustrates a typical TEG with its various components. The voltage generated (1) is directly proportional to the temperature difference between the top and bottom ceramic surfaces [2].

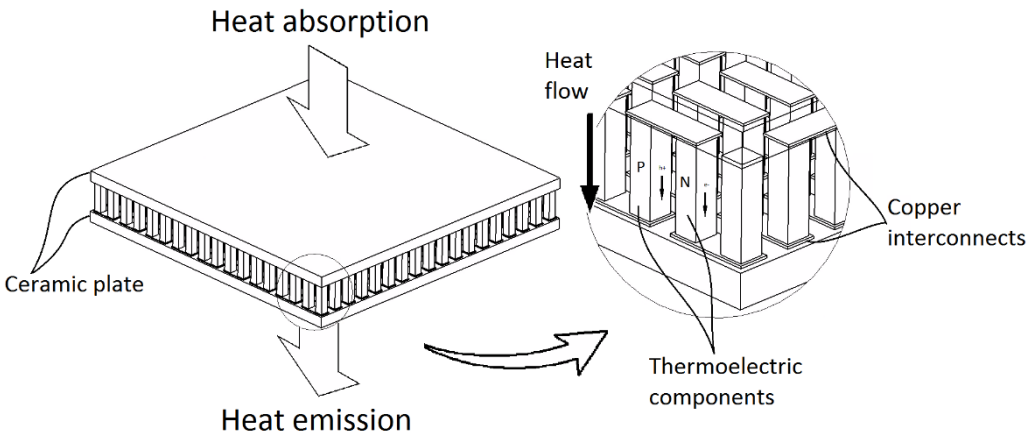

Figure 1:Structure of a TEG, visible are the thermocouples, the copper bridges and the ceramic plates

This report discusses development of a multi-physical simulation model of TEG using *ANSYS Workbench 18.0*. The final model is comparable to its commercial counterparts and can be used to simulate the working of a commercially available thermoelectric (TE) module for further analysis.

1.1 Basic TE module

A basic thermoelectric module works on the principle of Seebeck effect, The Seebeck effect can be simply schematized, where an applied temperature difference drives charge carriers in the material (electrons and/or holes) to diffuse from hot side to cold side, resulting in a potential difference through the circuit [3][4].

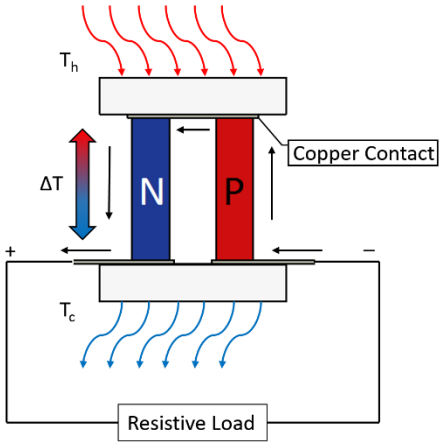

Figure 2:Simplified TE device showing the existence of a ΔT across the device

The assembly is made from an array of thermocouples consisting of p-type (hole transporting) and n-type (electron transporting) elements as shown in Figure 2. These are connected electrically in series with copper shunts and thermally in parallel. The outer endings are ceramic wafers to electrically insulate the thermocouple junctions. The magnitude of voltage output (1) is proportional to the Seebeck coefficient α, number of semiconductor thermocouples n and temperature difference. Using the output voltage the maximum power output can be calculated using the relation in equation (2) [5].

$$V_{out} = n \cdot \Delta T(\alpha_1 - \alpha_2) \tag{1}$$

$$P_{max} = \frac{V_{out}^2}{4R_{el}} \tag{2}$$

The performance of TE modules is measured using a dimensionless quantity called Figure of merit (ZT) (3). To obtain a high ZT, both Seebeck coefficient (α) and electrical conductivity (σ) must be large, while thermal conductivity (κ) must be minimized; however, due to the laws of physics this relation is not satisfied. For a thermoelectric device with two semiconductor materials the figure of merit is calculated using equation (4).

$$ZT = \frac{\sigma \alpha^2 T}{\kappa} \tag{3}$$

$$ZT = \frac{\left(\alpha_p + \alpha_n\right)^2 \overline{T}}{\left[\left(\rho_n \kappa_n\right)^{1/2} + \left(\rho_p \kappa_p\right)^{1/2}\right]^2} \quad (4)$$

1.2 Thermoelectric cooler as an alternative

The figure of merit for a TE module using Peltier effect for cooling has the same figure of merit as a power generation module using Seebeck effect [6]. Thus, at any given temperature, the best cooling material will also be the best material for generation. TEGs often are alike to TECs in physical form except that fewer, taller and thicker elements are used. The TEG has bigger but higher elements compared to TEC, Research suggests that for the power generation in the temperature range between 0 and 100 °C a TEC can be used in place of a TEG. For low temperatures, between 20 and 40 °C, the TEC is even a little better performing [7].

1.3 Intended application and motivation

Recent advances in thermoelectric research and the growing need of self-powered implants for the ageing populous has led to a growing interest in TEGs for energy harvesting applications. At present, most medical implant devices operate on lithium batteries which have a limited longevity [8]. TEGs on the other hand will operate using the unlimited energy sourced by harvesting the human body heat. The human body is a constant heat source and typically a temperature difference exists between muscle and the skin, even in a stationary scenario and/or during sleep, energy can be produced [9]. Electrically active implants having had success in clinical trials are gaining interest especially for regenerative therapies like regeneration of bone and cartilage, and implants for deep brain stimulation to treat movement disorders [10]. The ultimate goal of this model will be its induction in a hermetically sealed assembly to be used as an implantable medical device.

2 Choice of thermoelectric material

2.1 Material properties

Older thermoelectric devices typically used bi-metallic junctions, but newer TE devices generate electricity utilizing semiconductor materials such as Bismuth Telluride, Bi_2Te_3, which are good conductors of electricity, poor conductors of heat and exhibit large values of Seebeck coefficient [11]. These semiconductors are typically heavily doped to create an excess of electrons (n-type) or a deficiency of electrons (p-type).

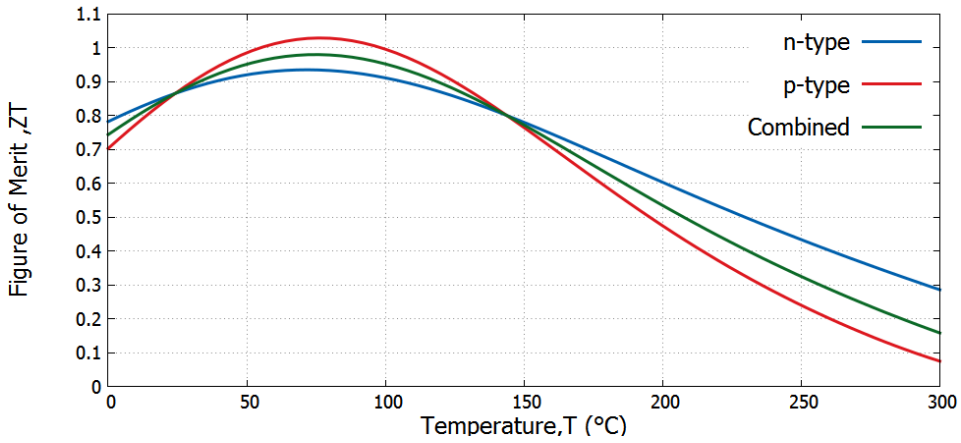

Figure 3:Figure of merit as a function of Temperature from (4)

The figure of merit of most thermoelectric materials are higher at temperatures well beyond ambient room temperature, Bi_2Te_3 on the other hand has a ZT value ranging from 0.8 to 1.0 at room temperature depending on the nanostructure and the doping [6]. This can also be illustrated from Figure 3, here the figure of merit of the device is given by the combined value calculated from equation (4). It is generally accepted that these alloys are the best available materials for generation as well as cooling near room temperature.

The following graphs exhibit the temperature dependency of Seebeck coefficient (Figure 4), Electrical conductivity (Figure 5), and thermal conductivity (Figure 6) [12].

For the insulated top and bottom pads for the TEG, a ceramic Al_2O_3 is used. These have high isotropic resistivity ($10^4\ \Omega m$) and low thermal conductivity ranging from 18-35 W/mK depending upon the purity (typically between 94 and 99.8%). The connections used to form a thermocouple are made from copper having high thermal conductivity (400 W/mK) and low isotropic resistivity (1.68 Ωm).

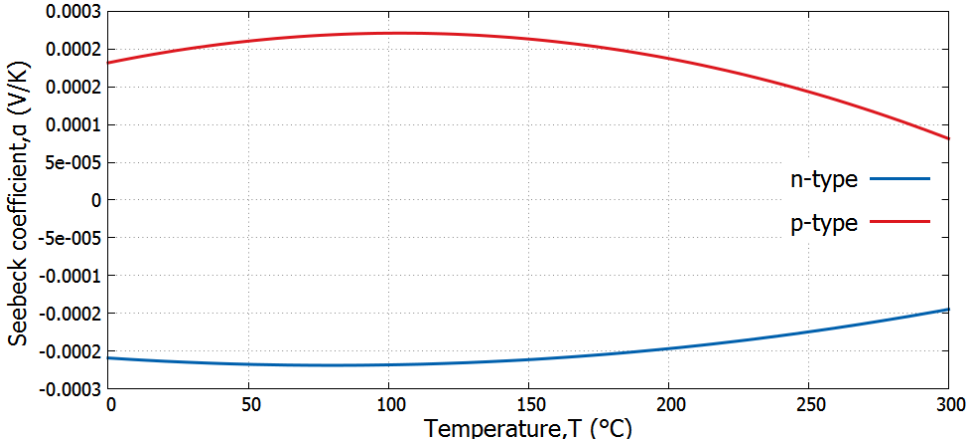

Figure 4:Seebeck coefficient as a function of Temperature from (7) & (8)

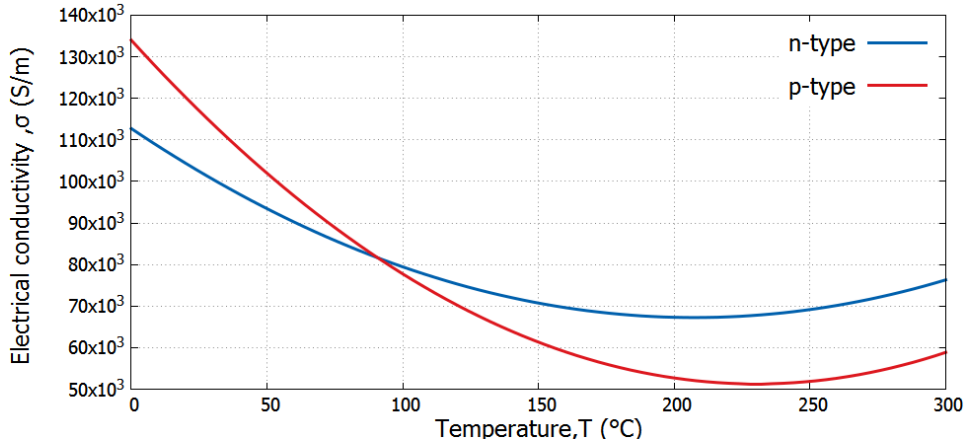

Figure 5:Electrical conductivity as a function of Temperature from (9) & (10)

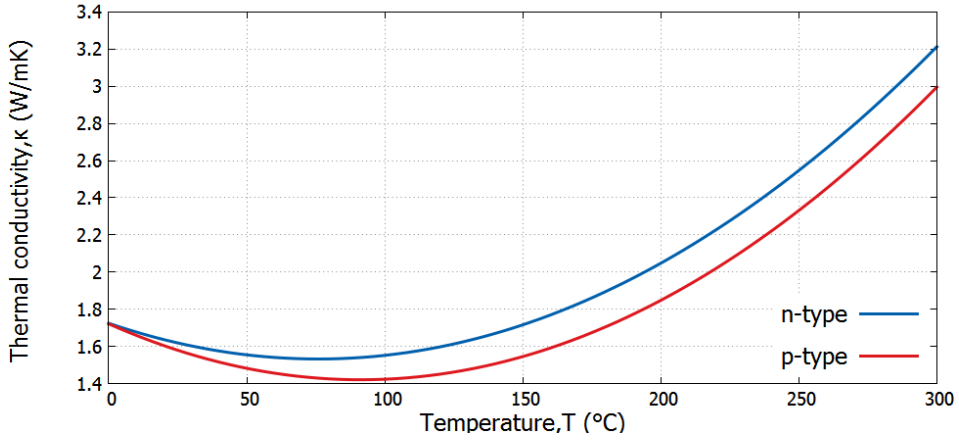

Figure 6:Thermal conductivity as a function of Temperature from (5) & (6)

3 Design

In a working thermoelectric device, elements of p-type and n-type doped semiconductor materials, are connected by electrical contacts to form a thermocouple. A voltage drives a current through the circuit, passing from one leg to another through the connecting copper contact. The geometry for TEGs and TECs is conceptually the same. In this case, the top side is connected to a heat source and the bottom to a heat sink.

3.1 Leg arrangement

A thermoelectric leg is a fundamental component of a TEG. A thermocouple formed by connecting two thermoelectric legs: one made of p-type and of one n-type semiconductor material which are connected in series electrically by a copper contact (Figure 2) and in parallel thermally.

To model the electrical contact in ANSYS Mechanical there are a number of ways, inserting a coupling between the faces of the legs, a simulating a surface contact of zero thickness and by modelling a physical contact. Inserting a couple between two elements while computationally less intensive increases the amount of manual work as the number of thermocouple increases, whereas a surface contact prevents having a singular part that leads to inaccurate results. On the other hand while having a physical contact increases the number of mesh elements it allows for a semi-automated approach for connections using the pattern feature in *DesignModeler*.

3.2 Parameters

Parameters are used for accelerated modification of the geometry for a different TE module without creating a new geometry. The current list of parameters control the various dimensions and pattern variables. Additional information for the respective parameter and the function is defined in Appendix 6.2 with the help of Table 3, Figure 19 and Figure 20.

3.3 Design process

The geometry for the multi-physical simulation is created using the *DesignModeler* in *ANSYS Workbench 18.0*, the process flow follows the sequence in Figure 7.

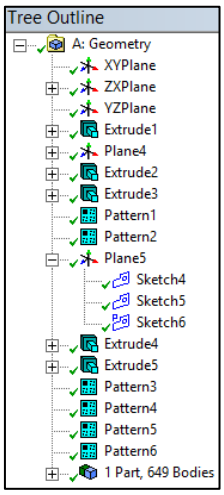

Figure 7:Design feature tree

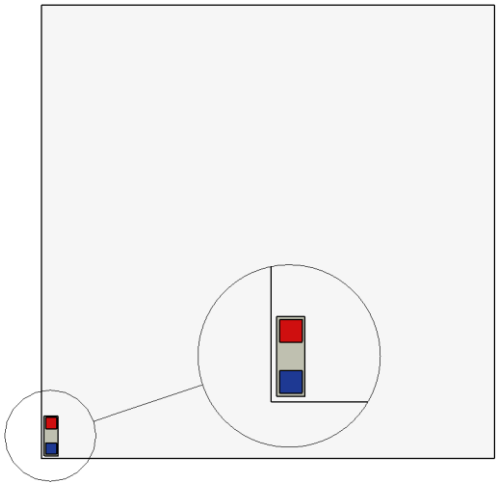

Figure 8:Generating the 1st thermocouple

Extrude 1 creates the bottom ceramic base of the required thickness, Extrude 2, 3 generate the thermocouple geometry with `vertical_pitch` between the p-type and n-type element (Figure 8).

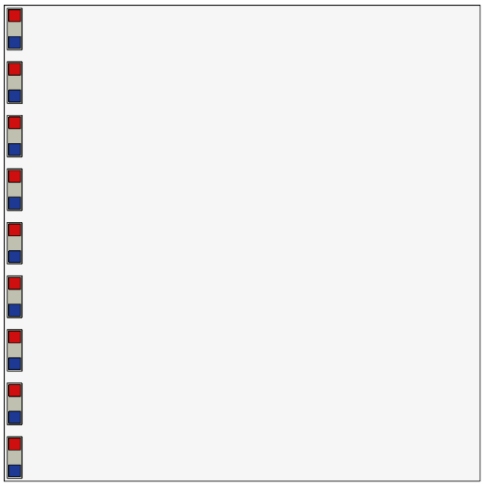

Figure 9:Pattern 1 in vertical direction

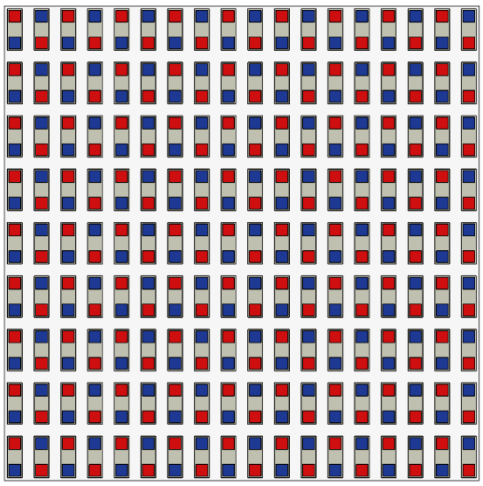

Figure 10:Pattern 2 in horizontal direction

Pattern 1 forms a linear pattern in vertical direction with the `vertical_pair_offset` and the `vertical_pair_num`, Pattern 2 forms a horizontal linear pattern with the new bodies (above).

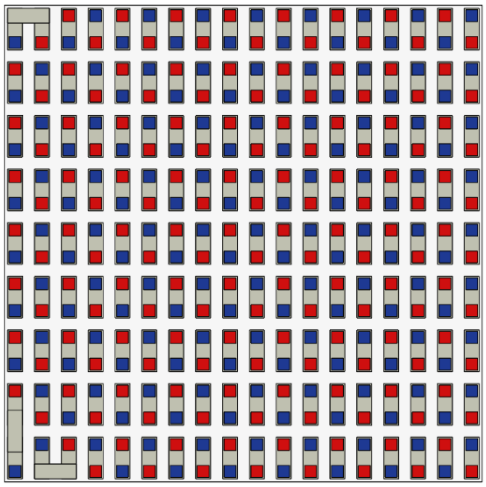

Figure 11:"Extrude 5" contacts for top connection

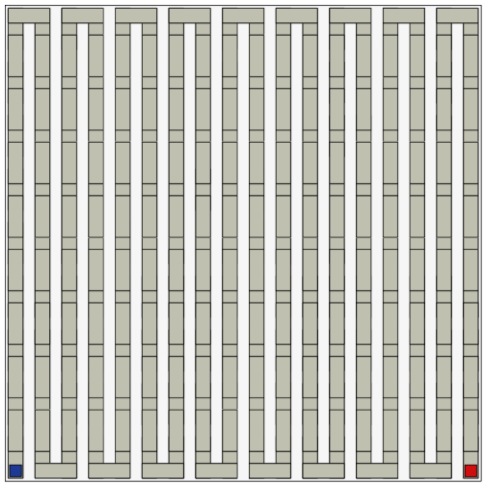

Figure 12: Pattern 3,4,5,6 for top contacts

On the top face of the elements, a plane is created to form the top ceramic cover using Extrude 4, the top copper contacts in Figure 11 are created by creating an equidistant perimeter around the sketch projection (Sketch 6) of connecting faces. Subsequent linear pattern form the contact pattern in Figure 12. Finally a single part is formed from all the Solid bodies to form a conforming mesh in *Mechanical* for further analysis.

4 ANSYS case setup

The *ANSYS Workbench* Project Schematic consists of Thermal-Electric, Steady-State Thermal and Electric simulations using a common Geometry, Mesh and Engineering Data.

4.1 Methodology

The geometry for the TEG is created using the process described in section 3.3. Engineering Data defines the material properties for the ceramic covers, p-type and n-type Bi_2Te_3 and copper contacts. The material properties for Bi_2Te_3 are inserted in Tabular form based on the temperature dependency in Appendix 6.1.

The geometry is attached in *Mechanical,* Individual bodies are grouped to assign the respective material properties. A coarse mesh is formed according to the default settings for minimizing the number of elements, this mesh is common for all three analyses. The results are compiled in Table 2 compared with commercial and analytical values.

4.2 Thermal-electric analysis

This is the main multiphysics simulation for comparing the TEG to its commercial counterpart. Thermal boundary conditions are set on the top and bottom faces of the cover as Hot-side and Cold-side temperature, and the electrical boundary condition is set as ground on top face of terminal element. Output voltage distribution is seen in Figure 14.

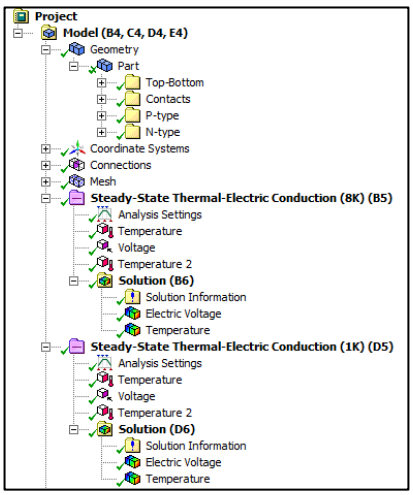

Figure 13: Project outline Thermal-electric

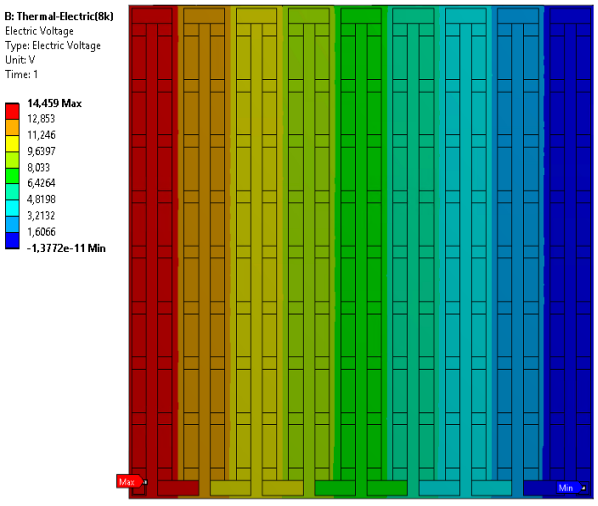

Figure 14:Electric Voltage distribution

4.3 Electric analysis

Electrical simulation with the given boundary conditions generates the electrical resistance of the TEG module. One terminal is set as ground while $1A$ current is supplied from the other terminal. The result is electric voltage distribution for electrical resistance, R_{el} (Figure 16).

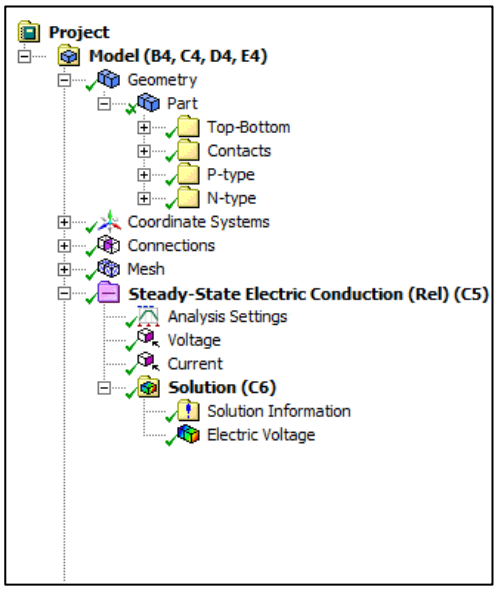

Figure 15:Project outline Electric analysis

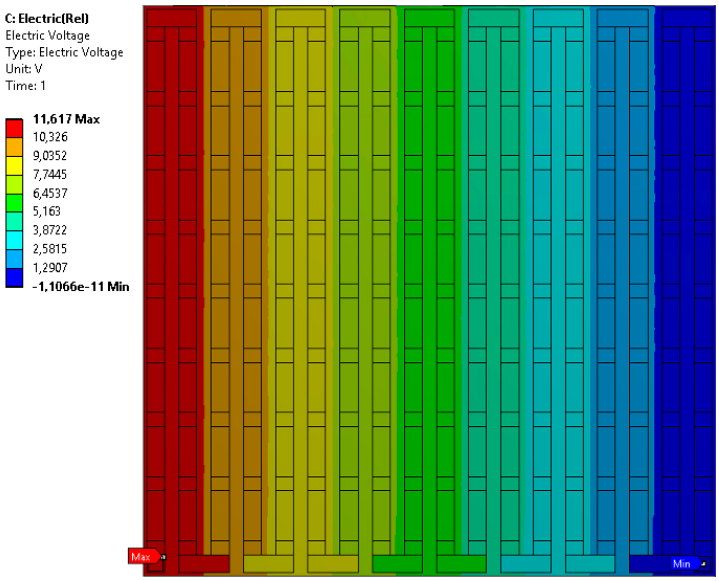

Figure 16:Electric Voltage distribution for Rel

4.4 Steady-state thermal analysis

Steady-state Thermal simulation is done to calculate the thermal resistance of the TEG module. The bottom surface of the module is thermally grounded (set at 0°C) and a heat flow of $1W$ is specified from the top surface inwards. Resultant temperature distribution provides the thermal resistance of the module (Figure 18).

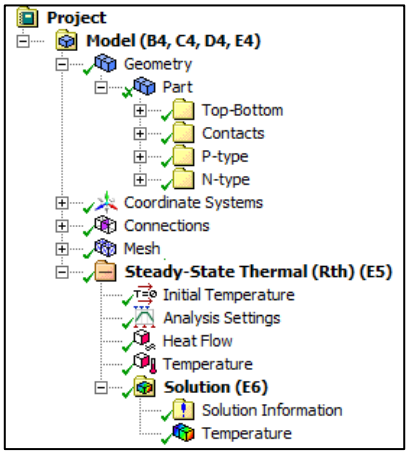

Figure 17:Project outline Steady-State Thermal analysis

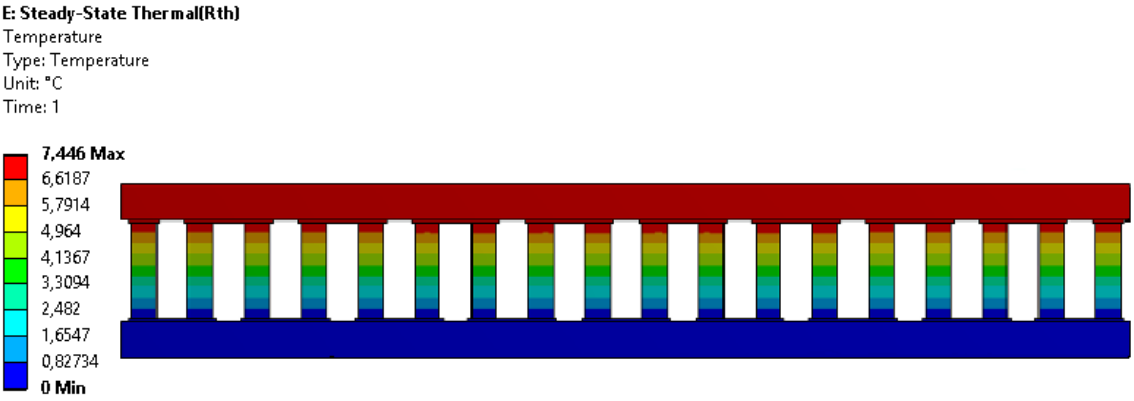

Figure 18:Temperature distribution for Rth

5 Results and Conclusion

This report has discussed the modeling and simulation of a thermoelectric generator module. The objectives of this project were to develop a comparable ANSYS model that closely replicates the physical device in operation. In this chapter, a summary of the work done and the results obtained after analysis are given.

5.1 Comparison with commercial TE modules

The voltage values from the simulation results vary by a small margin of error when compared to their rated voltage. From equation (2), the output power is proportional to V_{out}^2 , the presence of error in voltage thus affects the calculated power values.

The voltage and power output of a thermoelectric device scales with the number of couples for a given temperature difference, while the power density (power output per device area) is independent from the number of couples which is also observable from Table 2. The power output ultimately depends on the total device area, the element spacing, element length and material properties. The need for a large number of thermocouples within a small footprint requires high-density arrays of thermoelectric elements for a generator. In future, one could use this model to perform further analysis by integrating it in a much more complex system such as an electrically active biomedical implant.

Table 1: TE module with Manufacturer's data

	Manufacture's Data								
Model	**Dimensions**	**ΔT**	**N**	**t_{TEG}**	**A_{TEG}**	**Rated Voltage, $V\|_{\Delta T}$**	**Rated Voltage, $V\|_{1K}$**	**Electrical Resistance, R_{el}**	**Rated Power, P**
	mm	K		mm	mm^2	V	V	Ohm	W
Thermo-electric Generators									
GM250-161-12-40	40x40x6.8	220	324	3.8	1	12	0.05454	18.9	1.9
GM250-127-10-15	30x30x3.7	220	256	2	1	10.52	0.04781	6.89	4.02
Thermo-electric Coolers									
926-1027-ND	23x23x3.6	8	144	2.1	0.9604	-	-	-	-
926-1015-ND	25x25x3.42	8	256	2.06	0.6724	-	-	-	-

	Equivalent Circuit		ANSYS Model						
Model	**Electrical Resistance, R_{el}**	**Thermal Resistance, R_{th}**	**Rated Voltage, $V\|_{\Delta T}$**	**Rated Voltage, $V\|_{1K}$**	**Electrical Resistance, R_{el}**	**Thermal Resistance, R_{th}**	**Power$\|_{\Delta T}$**	**Power$\|_{1K}$**	**Power$\|_{1K}$/Area**
	Ohm	K/W	V	V	Ohm	K/W	W	µW	µW/mm2
@ 30 °C									
GM250-161-12-40	11.63059	7.499	14.459	0.06674	11.617	7.446	4.499067767	95.8471888	0.295824657
GM250-127-10-15	4.8963	5.016	11.359	0.05242	4.8451	5.3406	6.657596386	141.7853295	0.553848943
@ 27 °C									
926-1027-ND	2.9624	9.652	0.2337	0.02904	2.9396	10.463	0.004644823	71.72571787	0.518633135
926-1015-ND	7.34171	7.604	0.4218	0.05242	7.3235	8.1127	0.0060743	93.79196726	0.544876371

Table 2: Comparison of Equivalent circuit values with ANSYS model

References

[1] D. Champier, "Thermoelectric generators: A review of applications", *Energy Conversion and Management*, vol. 140, pp. 167-181, 2017.

[2] Y. Yang, X. Wei and J. Liu, "Suitability of a thermoelectric power generator for implantable medical electronic devices", *Journal of Physics D: Applied Physics*, vol. 40, no. 18, pp. 5790-5800, 2007.

[3] S. Riffat and X. Ma, "Thermoelectrics: a review of present and potential applications", *Applied Thermal Engineering*, vol. 23, no. 8, pp. 913-935, 2003.

[4] J. Li, W. Liu, L. Zhao and M. Zhou, "High-performance nanostructured thermoelectric materials", *NPG Asia Materials*, vol. 2, no. 4, pp. 152-158, 2010.

[5] M. Strasser, R. Aigner, M. Franosch and G. Wachutka, "Miniaturized thermoelectric generators based on poly-Si and poly-SiGe surface micromachining", *Sensors and Actuators A: Physical*, vol. 97-98, pp. 535-542, 2002.

[6] H. Goldsmid, "Bismuth Telluride and Its Alloys as Materials for Thermoelectric Generation", *Materials*, vol. 7, no. 4, pp. 2577-2592, 2014.

[7] M. Nesarajah and G. Frey, "Thermoelectric power generation: Peltier element versus thermoelectric generator", *IECON 2016 - 42nd Annual Conference of the IEEE Industrial Electronics Society*, 2016.

[8] V. PARSONNET and A. CHEEMA, "The Nature and Frequency of Postimplant Surgical Interventions:", *Pacing and Clinical Electrophysiology*, vol. 26, no. 12, pp. 2308-2312, 2003.

[9] M. Thielen, L. Sigrist, M. Magno, C. Hierold and L. Benini, "Human body heat for powering wearable devices: From thermal energy to application", *Energy Conversion and Management*, vol. 131, pp. 44-54, 2017.

[10] C. Watkins, B. Shen and R. Venkatasubramanian, "Low-grade-heat energy harvesting using superlattice thermoelectrics for applications in implantable medical devices and sensors", *ICT 2005. 24th International Conference on Thermoelectrics*, 2005.

[11] Bass, John C., "Thermoelectric Generator," *United States Patent 5892656,* 1999.

[12] "GM250-161-12-40, Thermoelectric generator module", European Thermodynamics. [Online].Available:http://www.europeanthermodynamics.com/products/datasheets/GM250-161-12-40%20(2).pdf.

6 Appendix

6.1 Temperature dependency of thermoelectric material properties

In this appendix, the relation of various material properties is defined with the operating temperature based on best fit derived from measured material characteristics from the module data sheet [12].

The respective curves for the material properties are available in Chapter 2.

Thermal Conductivity

$$k_n = (0.0000334545\,T^2 - 0.023350303\,T + 5.606333)\ W/mK \qquad (5)$$

$$k_p = (0.0000361558\,T^2 - 0.026351342\,T + 6.22162)\ W/mK \qquad (6)$$

Seebeck Coefficient

$$a_n = (0.001530736\,T^2 - 1.08058874\,T - 28.338095) \times 10^{-6}\ V/K \qquad (7)$$

$$a_p = (-0.003638095\,T^2 + 2.7438095\,T - 296.21428) \times 10^{-6}\ V/K \qquad (8)$$

Electrical Conductivity

$$\sigma_p = (0.015601732\,T^2 - 15.708052\,T + 4466.38095) \times 10^2\ S/m \qquad (9)$$

$$\sigma_n = (0.01057143\,T^2 - 10.16048\,T + 3113.71429) \times 10^2\ S/m \qquad (10)$$

6.2 Design parameters

In this appendix the design parameters discussed in section 3.2 are detailed. Table 3 lists all the parameters used for defining the sketch, the respective parameters are marked in Figure 19 and Figure 20.

Table 3: Design Parameters

Number	Parameter name	Value	Unit
1	module_side	40	mm
2	ceramic_thickness	1.4	mm
3	copper_thickness	0.1	mm
4	peltier_side	1	mm
5	vertical_pitch	1.25	mm
6	border_offset	0.375	mm
7	copper_peltier_offset	0.125	mm
8	peltier_height	3.8	mm
9	vertical_pair_offset	4.5	mm
10	vertical_pair_num	8	val
11	horizontal_pair_offset	2.25	mm
12	horizontal_pair_num	17	val

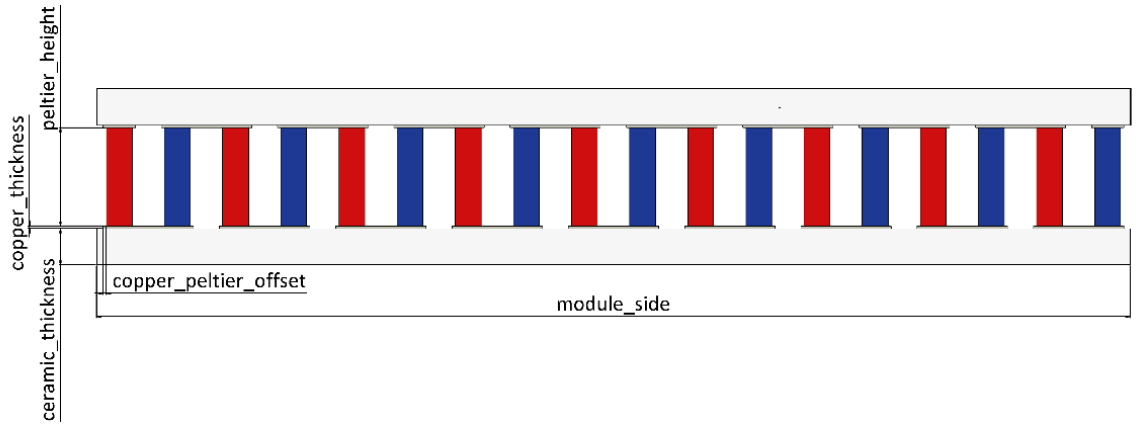

Figure 19:Pattern Schematic 1

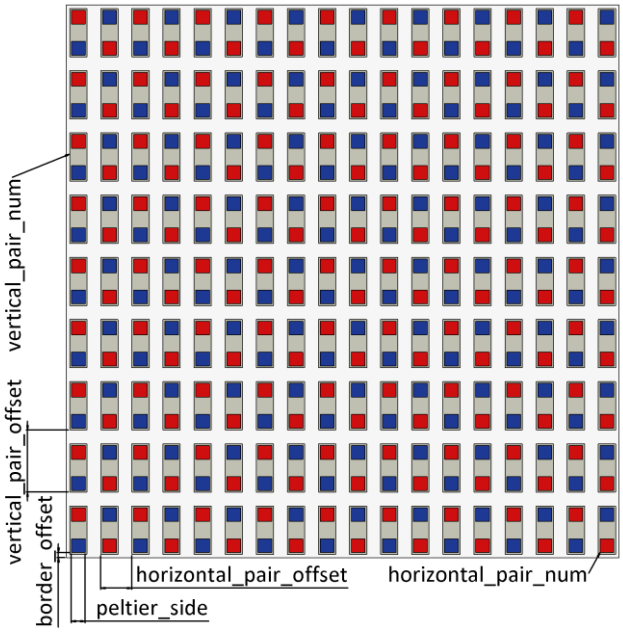

Figure 20: Pattern Schematic 2

6.3 Analytical calculations for resistance

In this section, the analytical calculations for the thermal and electrical resistances are shown.

6.3.1 Electrical resistance

For calculation of electrical resistance equation (11) is used based on the schematic in Figure 21, where N is the number of thermocouples and ρ is the resistivity of the respective material at operating temperature. The results respective to the TE modules are shown in Table 4

$$R_{el} = N \times \left(\left(\frac{h_{leg}}{A_{leg}} \times (\rho_p + \rho_n) \right) + 2 \left(\frac{x}{l \times h_{cu}} \times (\rho_{cu}) \right) \right) \tag{11}$$

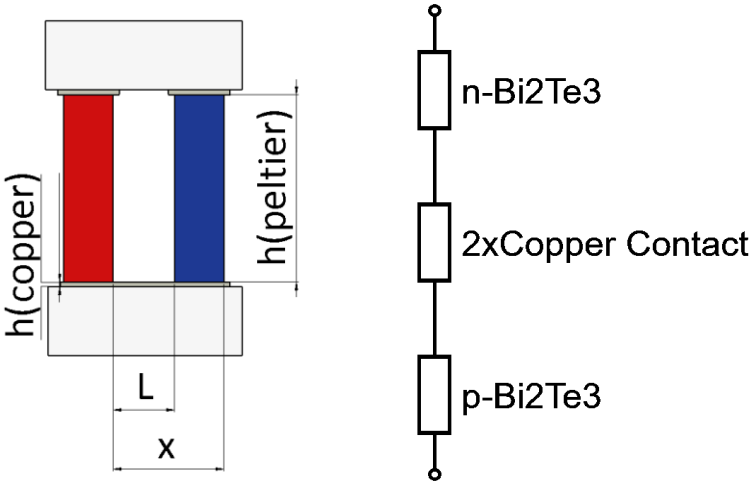

Figure 21:Reference schematic for electrical resistance

Table 4: Electrical resistance for TEG modules

TEG Module	R_{el} [Ω]
GM250-161-12-40 (18x18)	11.63
GM250-127-10-15 (16x16)	4.896
926-1015-ND (16x16)	7.342
926-1027-ND (12x12)	2.962

6.3.2 Thermal resistance

For calculation of thermal resistance equation (12) is used based on the schematic in Figure 22, where N' is the number of Peltier legs, κ is the thermal conductivity of the respective material at operating temperature and $\kappa_{mean,peltier}$ is the mean thermal conductivity of p-type and n-type Peltier element at operating temperature. The thermal resistances for the TE modules is shown in Table 5.

$$R_{th} = \frac{2}{\kappa_{Al_2O_3}}\left(\frac{h_{Al_2O_3}}{A_{Al_2O_3}}\right) + \frac{1}{N'}\left(\left(\frac{1}{\kappa_{mean,leg}}\left(\frac{h_{leg}}{A_{leg}}\right)\right) + 2\left(\frac{1}{\kappa_{cu}}\left(\frac{h_{cu}}{A_{cu,contact}}\right)\right)\right) \qquad (12)$$

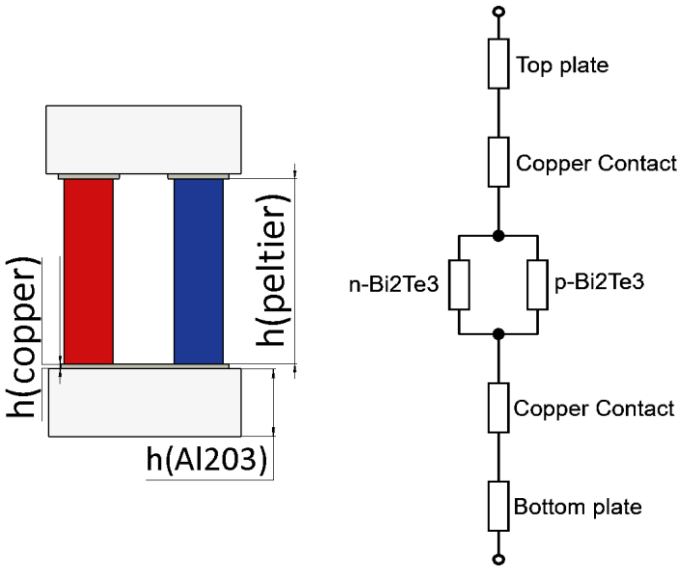

Figure 22:Reference schematic for thermal resistance

Table 5: Thermal resistance for TEG modules

TEG Module	R_{th} [K/W]
GM250-161-12-40 (18x18)	7.499
GM250-127-10-15 (16x16)	5.016
926-1015-ND (16x16)	7.603
926-1027-ND (12x12)	9.652